Feasibility study: Spot-scanning Proton Arc therapy (SPArc) for left-sided breast irradiation

Sheng Chang
Wuhan University Renmin Hospital
Gang Liu
Wuhan Union Hospital
Lewei Zhao
William Beaumont Hospital - Royal Oak
Joshua T Dilworth
William Beaumont Hospital - Royal Oak
Weili Zheng
William Beaumont Hospital - Royal Oak
Saada Jawad
William Beaumont Hospital - Royal Oak
Di Yan
William Beaumont Hospital - Royal Oak
Peter Chen
William Beaumont Hospital - Royal Oak
Craig Stevens
William Beaumont Hospital - Royal Oak
Peyman Kabolizadeh
William Beaumont Hospital - Royal Oak
Xiaoqiang Li
William Beaumont Hospital - Royal Oak
Xuanfeng Ding (xuanfeng.ding@beaumont.edu)
Beaumont Health System

Research

Keywords: spot scanning, proton arc, left-sided breast cancer, robustness optimization

Posted Date: July 2nd, 2020

DOI: https://doi.org/10.21203/rs.3.rs-38925/v1

Version of Record: A version of this preprint was published on October 7th, 2020. See the published version at https://doi.org/10.1186/s13014-020-01676-3.

Abstract

Background

This study investigated the feasibility and potential clinical benefit of utilizing a new proton treatment technique: Spot-scanning Proton Arc (SPArc) therapy for left-sided breast cancer irradiation to further reduce radiation dose to healthy tissue and mitigate the probability of normal tissue complications compared to conventional Intensity Modulated Proton Therapy(IMPT).

Methods

Eight patients diagnosed with left-sided breast cancer and treated with breast-preserving surgery followed by whole breast irradiation without regional nodal irradiation were included in this retrospective planning. Two proton treatment plans were generated for each patient: vertical intensity-modulated proton therapy used for clinical treatment (vIMPT, gantry angle 10°-30°) and SPArc for comparison purpose. Both SPArc and vIMPT plans were optimized using the robust optimization of ± 3.5% range and 5 mm setup uncertainties. Root-mean-square deviation dose (RMSD) volume histograms were used for plan robustness evaluation. All dosimetric results were evaluated based on dose-volume histograms (DVH), and the interplay effect was evaluated based on the accumulation of single-fraction 4D dynamic dose on CT50. The treatment beam delivery time was simulated based on a gantry rotation with energy-layer-switching-time (ELST) from 0.2 to 5 s.

Results

The average D1 to the heart and LAD were reduced to 53.63 cGy and 82.25 cGy compared with vIMPT 110.38 cGy (p = 0.001) and 170.38 cGy (p = 0.001), respectively. The average V5Gy and V20Gy of ipsilateral lung was reduced to 16.77% and 3.07% compared to vIMPT 25.56% (p = 0.001) and 4.68% (p = 0.003). Skin3mm mean and maximum dose was reduced to 3999.38 cGy and 4395.63 cGy compared to vIMPT 4104.25 cGy (p = 0.039) and 4411.63 cGy (p = 0.043), respectively. A significant relative risk reduction (RNTCP = NTCPSPArc / NTCPvIMPT) for organs at risk (OARs) was obtained with SPArc ranging from 0.61 to 0.86 depending on the clinical endpoint. The RMSD Volume Histogram(RVH) analysis shows SPArc provided better plan robustness in OARs sparing, including the heart, LAD, ipsilateral lung, and skin. The average estimated treatment beam delivery times were comparable to vIMPT plans when the ELST is about 0.5 s.

Conclusion

SPArc technique can further reduce dose delivered to OARs and the probability of normal tissue complications in patients treated for left-sided breast cancer.

Introduction

Breast cancer is one of the most common cancers among women globally [1]. Breast-conserving surgery with adjuvant whole breast irradiation has become an increasingly popular treatment option for early-stage breast cancer [2–6]. Currently, conventional photon treatment methods such as tangential intensity-modulated radiation therapy (IMRT) and volumetric-modulated arc therapy (VMAT) have offered increased feasibility for normal tissue sparing in left-sided breast irradiation [7–9]. However, long-term follow-up data after adjuvant radiotherapy have shown increased risks of ischemic heart disease, presumably due to incidental irradiation of the heart. Left-sided breast irradiation involves closer proximity between the heart and radiation field and is associated with an increased rate of fatal cardiovascular events [5, 6, 10, 11]. Part of the anterior heart and left anterior descending artery (LAD) may receive significant dose during irradiation of the left-sided breast, and this may contribute to myocardial or coronary artery disease [12]. Darby et al. showed linear correlation between increasing mean heart dose and the incidence of ischemic heart disease among breast cancer patients [13]. Additionally, similar studies have shown that breast cancer patients are at a higher risk of long-term cardiac morbidity after radiation therapy treatment, which is directly related to the volume of the irradiated heart [5, 6]. Therefore, the optimization of breast cancer radiotherapy has given increasing emphasis on reducing the cardiac dose.

Compared to photon radiotherapy, proton beam therapy may provide a dosimetric advantage whentreating left-side breast cancer due to the sharp distal dose fall-off of the proton beam. Utilization of intensity modulated proton therapy (IMPT) for breast cancer treatment has increased over the last several years [14–16]. In IMPT, the positions and number of beam spots are optimized simultaneously to obtain the desired dose distribution, and robust optimization has been used to deal with uncertainties such as setup uncertainty, range uncertainty, and breathing motion uncertainty [17–22]. However, due to the low delivery efficiency with the current proton system, IMPT plans in breast cancer are still limited to a few beam angles. In addition, a large volume of the target may exceed the maximum field size. As a result, some IMPT plans may require a second isocenter for field matching [23], which further prolongs treatment time. These obstacles restrict the ability to further exploit the benefits of IMPT, and motivates us to explore better planning techniques to overcome the current limitations in terms of plan quality and clinical workflow efficiency. Spot-scanning proton arc therapy (SPArc) is an emerging technique that is able to deliver the proton beam through a dynamic rotational gantry [24]. Preliminary results demonstrated the potential clinical benefits for various disease sites, including prostate, head and neck, lung, and brain cancers [25–28]. This study is the first to exploit the feasibility and potential benefits of utilizing SPArc in the treatment of left-sided breast cancer patients compared to the conventional IMPT technique.

Methods

Retrospective patient data selection and treatment planning

Eight patients treated with whole breast irradiation without regional nodal irradiation from our institution using IMPT were included in this study. All patients underwent 4D-CT simulation using a spiral CT scanner (Philips Brilliance Big Bore, Philips Healthcare System, Cleveland, OH), and an average CT image was reconstructed based on a pixel-by-pixel averaging of the 4D-CT scan. The CT datasets were then transferred to RayStation version 9A (RaySearch Laboratories AB, Stockholm, Sweden) for planning. Clinical target volume (CTV) was defined as the volume irradiated based on the Radiation Therapy Oncology Group (RTOG) guidelines [29]. The internal target volume (ITV) was generated on the average CT scan, which was the union of the CTVs from all individual respiratory phase CT scans. Two separate treatment plans were created for each case: vertical IMPT (vIMPT, 10°-30°) and SPArc (partial-arc) plans. Three of the patients with large tumors required two-isocenter IMPT plan due to the field size limitation (20 cm x 24 cm maximum field size). SPArc plans used a single isocenter with a partial arc. Both planning strategies used ITV plus robustness optimization to take into account setup (± 5 mm) and range (± 3.5%) uncertainties (total 21 scenarios). A standard deviation of 1.0% was used in Monte Carlo (MC) dose calculation with a dose grid of 3.0 mm. Organs at risk (OARs) include heart, LAD, ipsilateral lung, contralateral breast and skin3mm. The skin3mm was defined as a 3 mm deep layer starting from the external body contour and following the extension of the ITV. The prescribed dose for all patients was 4256 cGy in 16 fractions [30, 31]. Plans aimed to achieve 100% of the prescribed dose in 98% of the ITV. SPArc and vIMPT plans were optimized in Raystation TPS in similar objectives and constraints for OARs. The objective and constrain functions were specified individually for each patient to obtain the best achievable treatment plan until there is no significant improvement.

Nominal dosimetric Plan quality evaluation and plan robustness analysis

Target coverage and doses to OAR's were all evaluated and compared based on the DVH between SPArc and vIMPT. Also, the plan dose homogeneity was evaluated by homogeneity index (HI), which was defined as D_5/D_{95} (where D5 and D95 are the minimum dose in 5% and 95% of the target volume). The ideal value of HI is 1. ITV coverage was evaluated by the conformality index (CI), which was defined as CI= (TVDp/TV)*(TVDp/VDp), where the TV is target volume, and TVDp and VDp are the target volume covered by the prescribed dose, and the volume enclosed by the prescription isodose line, respectively [32]. The plan robustness was defined by the ability of a proton plan to retain its objectives under the influence of uncertainties. In the present study, all plans were evaluated using worst case scenario perturbed dose with setup uncertainties of ± 5 mm for x, y, z directions, and ± 3.5% range uncertainties. Besides, the root-mean-square deviation doses (RMSD) for each voxel of all the 21 scenarios were calculated. The RMSD volume histograms (RVH) and the area under the RVH curve (AUC), which introduced by Liu et al. were computed for relative comparison of IMPT and SPArc plan robustness [33]. The smaller the AUC value, the more robust the plan was for the specific structure(s).

Evaluation of motion interplay effect

The interplay effect was evaluated by the single-fraction 4D dynamic dose calculation without considering re-scanning for different starting respiratory phases [34]. This 4D dynamic dose calculation used a method by relating the time sequence of each spot delivery to the corresponding 4D-CT phase from the patient breathing cycle. Then it accumulated each spot dose via the deformable image

registration on the corresponding respiration phase to the reference 4D-CT phase (CT50) for evaluation, assuming the energy-layer-switching-time (ELST) of 1 s and a regular respiratory breathing cycle of 4.5 s.

Treatment beam delivery time calculation and statistics analysis

The treatment delivery efficiency of SPArc and vIMPT plans were evaluated based on assumptions of a gantry with 1 rotation per minute gantry speed, 2 ms spot switching time, and ELST from 0.2 to 5 s [24]. Statistical analysis was performed with non-parametric Wilcoxon signed rank test using SPSS 21.0 software (International Business Machines, Armonk, New York). The p-value < 0.05 was considered statistically significant.

Evaluation of Potential clinical benefit for OARs based on the NCTP model

Potential clinical benefits of each OAR such as heart, LAD, left lung, and skin were estimated using the normal tissue complication probability (NTCP) model from the literature (Table 1). Briefly, Lyman–Kutcher–Burman (LKB) and Possion LQ models were employed [35–39]. To compare risk values between SPArc and vIMPT plans, we defined the ratio of NTCP (R_{NTCP}), as $R_{NTCP} = NTCP_{SPArc} / NTCP_{vIMPT}$.

Table 1. OARs, corresponding clinical endpoints, and NTCP models used in the present work.

OAR	Clinical endpoint	Reference	Model
Heart	Mortality	Gagliardi et al. (1996) [35, 39]	Poission LQ model:D50=52.4Gy,γ=1.28,s=1
LAD	Mortality	Gagliardi et al. (1996) [35, 39]	Poission LQ model:D50=52.4Gy,γ=1.28,s=1
Left lung	Radiation pneumonitis	Seppenwoolde et al. (2003) [37, 38]	LKB model: TD50 = 30.8 Gy, m = 0.37, n = 0.99
Skin	Severe acute toxicity	Pastore et al. (2016) [36, 38]	LKB model: TD50=39 Gy, m=0.14, n=0.38

Abbreviations: LKB model: $NTCP=\frac{1}{\sqrt{2\pi}}\int_{-\infty}^{t} e^{-t^2/2}\,dt$, t=(D-$TD_{50}$(V))/(m·$TD_{50}$(V)), $TD_{50}(V)=TD_{50}(1)/V^n$

Poission LQ model: $NTCP=\{1-\prod_{i=1}^{n}[1-P(D_i)^s]^{V_i/V}\}^{1/s}$, $P(D_i)=2^{-exp\{e\gamma(1-D_i/D_{50})\}}$

Results

Nominal Dosimetric plan quality comparisons

Figure 1 shows an example (patient #5) of radiation treatment plans and DVHs for SPArc and vIMPT. With a similar target coverage (Table 2), the SPArc technique achieved significantly higher dose homogeneity compared with the vIMPT technique (p < 0.001). Specifically, SPArc plans showed a significant reduction in heart dose (D1) of 51.42% compared to vIMPT (53.63 cGy vs 110.38 cGy, p = 0.001), as well as a substantial decrease in the maximum dose to LAD of 51.72% (82.25 cGy vs 170.38 cGy, p = 0.001). Compared to vIMPT, the volume of left lung received 500 (cGy) and 2000 (cGy) was reduced by 34.40% (16.77% vs 25.56%, p = 0.001) and 34.51% (3.07% vs 4.68%, p = 0.003) via SPArc. The skin3mm structure mean and maximum dose was reduced to 3999.38 cGy and 4395.63 cGy compared to vIMPT plans (4104.25 cGy (p = 0.039) and 4411.63 cGy (p = 0.043)) respectively. However, the study found that the mean dose of the contralateral breast was increased to 18.5 cGy in the SPArc plans compared to the vIMPT plans (12.13 cGy, p = 0.011).

Table 2
Target volume and OARs dosimetric parameters for vIMPT and SPArc

Structure	Value	SPArc			vIMPT			Relative difference		
		Planned	4D dynamic dose	AUC	Planned	4D dynamic dose	AUC	Planned	4D dynamic dose	AUC
ITV	D98(cGy)	4256	4262.75 ± 3.62	64.5 ± 15.55	4256	4265.63 ± 7.89	64.5 ± 5.73	-	2.88 ± 9.89 (p = 0.438)	0 ± 13.54 (p = 1)
HI		1.05 ± 0.01	1.05 ± 0.01		1.08 ± 0.02	1.07 ± 0.02		0.03 ± 0.02 (p = 0.005)	0.03 ± 0.02 (p = 0.006)	
CI		0.78 ± 0.06	0.79 ± 0.05		0.77 ± 0.06	0.77 ± 0.05		-0.02 ± 0.02 (p = 0.044)	-0.02 ± 0.02 (p = 0.018)	
heart	D1(cGy)	53.63 ± 18.19	56.88 ± 19.90	2.25 ± 0.89	110.38 ± 18.93	126.88 ± 26.25	4.00 ± 1.51	56.75 ± 34.08 (p = 0.001)	70.00 ± 32.14 (p < 0.001)	1.75 ± 1.39 (p = 0.009)
	Mean Dose(cGy)	4.5 ± 2.33	4.75 ± 2.31		6.38 ± 2.13	6.75 ± 2.05		1.88 ± 2.10 (p = 0.04)	2.00 ± 2.07 (p = 0.029)	
LAD	D1(cGy)	82.25 ± 37.38	87.38 ± 40.29	9.88 ± 3.68	170.38 ± 74.31	196.5 ± 61.57	21.25 ± 10.35	88.13 ± 49.66 (p = 0.001)	109.13 ± 57.17 (p = 0.001)	11.38 ± 9.29 (p = 0.01)
contralateral breast	Mean Dose(cGy)	18.5 ± 7.07	19.75 ± 8.01	4.75 ± 2.31	12.13 ± 2.70	11.88 ± 3.40	3.63 ± 2.45	-6.37 ± 5.89 (p = 0.011)	-7.88 ± 6.73 (p = 0.013)	-1.13 ± 2.53 (p = 0.249)
ipsilateral lung	V500(cGy)	16.77 ± 7.18	16.63 ± 7.13	122.63 ± 38.26	25.56 ± 5.95	25.73 ± 5.27	168.25 ± 29.05	8.79 ± 5.25 (p = 0.001)	9.11 ± 5.28 (p = 0.002)	45.63 ± 21.54 (p = 0.001)
	V2000(cGy)	3.07 ± 2.17	3.06 ± 2.12		4.68 ± 1.78	4.67 ± 1.77		1.61 ± 1.03 (p = 0.003)	1.61 ± 1.04 (p = 0.003)	
	Mean dose(cGy)	282.75 ± 128.73	280.29 ± 127.59		395.38 ± 91.19	400.69 ± 94.82		112.63 ± 88.06 (p = 0.009)	120.40 ± 77.92 (p = 0.003)	
Skin3mm	D1(cGy)	4395.63 ± 98.35	4386.25 ± 96.62	85.5 ± 11.71	4411.63 ± 72.03	4402.5 ± 107.87	81.25 ± 27.73	16.00 ± 113.86 (p = 0.043)	16.25 ± 113.92 (p = 0.05)	-4.25 ± 21.10 (p = 0.587)
	Mean Dose(cGy)	3999.38 ± 120.57	3992 ± 108.02		4104.25 ± 110.34	4097.75 ± 90.84		104.87 ± 115.17 (p = 0.039)	105.75 ± 112.03 (p = 0.032)	

Abbreviations: ITV internal target volume, HI homogeneity index, AUC area under the curve.

Plan robustness evaluation in the presence of the setup&range uncertainties

All the AUC values of target volumes and OARs from eight cases were evaluated. Compared to vIMPT plans, the robustness OARs dosimetric were significantly improved in SPArc plans such as heart (4.00 in vIMPT plan versus 2.25 in SPArc plan, p = 0.009), left-lung (168.25 in vIMPT versus 122.63 in SPArc, p = 0.001) and LAD (21.25 in vIMPT versus 9.88 in SPArc, p = 0.01). There is no statistical difference in contralateral-breast and skin3mm's dosimetric robustness. Figure 2 illustrates RVHs from case number 5.

Evaluation of dosimetric impact from the interplay Effect

The study found that SPArc could improve the plan robustness in both target and OARs (Table 1), where the SPArc was able to maintain the HI of dose (1.05 vs 1.07, p = 0.006) and the CI of ITV (0.79 vs 0.77, p = 0.018). In addition, SPArc plans were able to mitigate the dose perturbation in the heart (22.75 cGy vs 68.38 cGy p < 0.001) and left lung (39.50 cGy vs 94.50 cGy p = 0.003) from the interplay effect significantly. Figure 3 shows a representative example of the 4D dynamic dose calculation of SPArc versus vIMPT plans.

Beam delivery efficiency

Table 3 lists the estimated beam delivery time per fraction for both SPArc and vIMPT plans for various ELST. When the proton system's ELST is 5 s, the average estimated delivery time ratios between SPArc and vIMPT plans was 1.40 (1059s vs. 758 s), which means it would take significantly longer to deliver a SPArc plan (p < 0.001). The difference became smaller as the ELST is faster. When the ELST was less than 0.5 s, the treatment delivery time of SPArc plan could be less than vIMPT (p = 0.005) (Fig. 4). However, the estimated treatment time didn't take into account the additional time to perform iso-shift and re-imaging. For the 2-isoenter vIMPT plan, additional couch movement for the next iso and IGRT verification procedures may be needed to ensure the treatment accuracy. For SPArc, only a single iso is needed, which would save significant additional treatment time as well as simplify the clinical treatment workflow.

Table 3
Plan parameter comparison between vIMPT and SPArc

Plan parameters	vIMPT	SPArc	Relative difference
Beam directions	1	39	38
Total energy layers	27 ± 3.85	93 ± 4.57	66 ± 6.95
Total monitor unit	6143 ± 1281.08	5511 ± 1233.95	-633 ± 140.91
Total delivery time(5 s)	758 ± 144.17	1059 ± 123.77	301 ± 30.34(p < 0.001)
Total delivery time(4 s)	732 ± 141.3	967 ± 126.08	235 ± 24.17(p < 0.001)
Total delivery time(3 s)	706 ± 138.53	874 ± 128.50	169 ± 18.41(p < 0.001)
Total delivery time(2 s)	680 ± 135.79	782 ± 131.04	102 ± 13.64(p < 0.001)
Total delivery time(1 s)	654 ± 133.11	690 ± 133.68	36 ± 11.18(p < 0.001)
Total delivery time(0.5 s)	641 ± 131.79	644 ± 135.03	3 ± 11.35(p = 0.47)
Total delivery time(0.2 s)	633 ± 131.00	616 ± 135.86	-17 ± 11.93(p = 0.005)

Potential clinical benefit for heart

The results show that there was a potential clinical benefit based on NTCP model calculation of using SPArc over vIMPT (Table 4). More specifically, heart, LAD, left-lung, and skin complications showed an overall reduction in the toxicity risk prediction for SPArc plans compared with the vIMPT plan, with R_{NTCP} ranging from 0.61 to 0.86, depending on the clinical endpoint (Fig. 5).

Table 4
R_{NTCP} ratio comparison according to normal tissue complication probability (NTCP) analysis for heart, LAD, skin and lung.

		Median (range)	
OAR	Clinical endpoint	$R_{NTCP} = NTCP_{SPArc} / NTCP_{vIMPT}$	P-value
heart	Major coronary events	0.77(0.59–0.96)	0.003
LAD	Coronary stenosis	0.69(0.45–1.01)	0.119
Left lung	Radiation pneumonitis	0.86(0.57–0.95)	0.005
Skin	Severe acute toxicity	0.61(0.35–0.78)	0.007

Discussion

This is a first and comprehensive dosimetric planning study to explore the feasibility and potential dosimetric and clinical benefits in the management of patients with left-sided breast cancer receiving whole breast irradiation. This study also analyzed plan robustness in the presence of setup and range errors in addition to the breathing-induced interplay effect. Our results indicate that the SPArc technique with additional degree of freedom in optimization and delivery could not only improve dosimetric quality but also improve plan robustness compared to conventional vIMPT.

The results from this study agree with previous findings that SPArc could shorten the total treatment delivery time based on the modern proton therapy machines where the average of ELST is less than 0.5 s [25–28, 40]. In the presence of the larget target size, which requires multi-isoenter field matching, SPArc technique could utilize a single-isoenter to simplify the clinical treatment workflow. For example, three out of eight cases included in this study required a second isocenter. As a result, therapists need to apply an isocenter shift, image validation, and second treatment field in the vIMPT treatment. A review of treatment logs of these three cases found that it took 5.11 ± 0.05 min on average to perform these additional procedures for the 2nd isocenter shift. These additional couch isocenter shift and image acquisition times prolong the overall treatment time and also increase the chance of intrafraction motion [41–43]. Thus, SPArc has the potential to provide a more efficient clinical treatment workflow through one arc trajectory and further reduce the uncertainties from the intrafraction motion.

Cardiac toxicityremains a leading treatment related cause of morbidity and mortality among long-term breast cancer survivors after radiotherapy, especially in the patient population with left-sided breast cancer [44]. Previous studies have found several heart dosimetric metrics related to acute or late cardiotoxicity, although there are still debates in which dosimetric metric and substructures are more related to the acute or late cardiotoxicity [45–48].

Darby et al. found that the rate of the incidence of ischemic heart disease increased linearly with the mean heart dose by 7.4% per Gy [13]. In addition, the RADCOMP (Radiotherapy Comparative Effectiveness) trial has also pointed out that the mean heart dose as a critical indicator for cardiotoxicity [45, 49]. The mean heart dose of the delivered vIMPT plans in our study was 6.38 cGy, which is higher than SPArc 4.5 cGy ($p = 0.04$). Moreover, there is increasing evidence that the dose of heart substructures needs to be considered. Some studies have focused on the LAD as important parts of the heart associated with radiation-induced heart disease [11, 50]. Conventional proton beam therapy (IMPT or Passive-scattering) could reduce the dose of the heart and LAD in left-side breast cancer patients compared to the photon radiotherapy technique in the high cardiac doses sparing [10, 15, 51]. This study found that the new proton treatment technique, SPArc, could further reduce the D1 of heart and LAD which might mitigate the probability of heart acute and late toxicities. We recognize that the relevance of photon NTCP models to proton therapy has not been established and further proton study would be needed to correlate the proton dose with the cardiotoxicity. The study also found that the contralateral breast mean doses were slightly higher in SPArc planning group compared with vIMPT. It is important to consider and choose the optimal treatment technology for an individual patient considering the possible clinical benefits as well as the limitation of using SPArc technique.

Another critical OAR that could benefit from SPArc is the healthy lung tissue. Reducing the radiation dose to the lung can result in reducing the risk of radiation pneumonitis in patients. Our feasibility study finds that the technology of SPArc can substantially improve not only the heart and LAD sparing but also the lung sparing in comparison with vIMPT. Previous studies have confirmed that proton therapy can significantly reduce the V500(cGy) and V2000(cGy) of the ipsilateral lung by nearly 50% compared to traditional 3DCRT and IMRT [10, 52, 53]. This study found that SPArc plans further reduced all dose-volume parameters while providing a reduced or similarly high-dose radiation volume with IMPT in left-sided breast cancer.

Conclusions

SPArc can achieve superior OARs sparing and robust plan quality in left breast irradiation compared to the traditional IMPT. With ELST less than 0.5 s in current modern proton systems, the total beam delivery time per fraction of SPArc would be faster than IMPT which would be desirable for future clinical implementation.

Abbreviations

LAD: left anterior descending; IMPT: Intensity Modulated Proton Therapy; SPArc: Spot-Scanning Proton Arc; vIMPT: vertical intensity-modulated proton therapy; RMSD: Root-mean-square deviation dose; DVH: Dose Volume Histogram; ELST: Energy-Layer-Switching-Time; D1: Dose received by 1% of volume; IMRT: Intensity Modulated Radiation Therapy; VMAT: volumetric modulated arc therapy; RTOG: Radiation Therapy Oncology Group; ITV: internal target volume; MC: Monte Carlo; HI: homogeneity index; CI: conformality index;

D5: Dose received by 5% of volume; D95: Dose received by 95% of volume; RVH: RMSD volume histograms; AUC: Area Under the RVH curve; OARs: Organ at risks; NTCP: normal tissue complication probability; LKB: Lyman–Kutcher–Burman; RADCOMP: Radiotherapy Comparative Effectiveness; V500: Volume received at least 500cGy; V2000: Volume received at least 2000cGy

Declarations

Acknowledgements

This study in part is supported by from Ion Beam Application S.A. research grant, Herb and Betty Fisher Research Seed Grand Award from Beaumont Health.

Funding

The study is supported by research funding from Ion Beam Application S.A. (Louvain-la-Neuve, Belgium) and Beaumont Health Herb and Betty Fisher Research Seed Grant Award.

Availability of data and materials

All data generated or analyzed during this study are included in this published article. Additional information is available from the corresponding author on reasonable request.

Authors' contributions

SC and GL contribute to the acquisition, analysis and interpretation of the result and draft and design the paper. PK WZ, SJ, PC, CS and JD provided clinical inputs; DY and LZ provide imaging acquisition and support and statistical analysis; XL provided technical support. XD, contribute to the design of the study, revise the draft and lead the research direction. All authors read and approved the final manuscript.

Ethics approval and consent to participate

The patient data used in this study is approved by Beaumont institutional IRB.

Consent for publication

Not applicable.

Competing interests

Xuanfeng Ding, Xiaoqiang Li and Di Yan has a patent related to the Spot-scanning proton arc (SPArc). The patent has been licensed to Ion Beam Application.

Disclosure:

X.D. reports personal fee from Ion Beam Applications' Speaker Bureau. P.K. reports personal fee from Ion Beam Applications' Speaker Bureau

Author details

[1]Department of Radiation Oncology, Wuhan University, Renmin Hospital, Wuhan, 430060 Hubei Province, China

[2]Department of Radiation Oncology, Beaumont Health System, Royal Oak, MI 48074, USA.

[3]Cancer Center, Union Hospital, Tongji Medical College, Huazhong University of Science and Technology, Wuhan 430023, China.

[4] School of Physics and Technology, Wuhan University, Hubei, Wuhan 430072, China.

References

1. International Agency for Research on Cancer. Latest world cancer statistics Global cancer burden rises to 14.1 million new cases in 2012: Marked increase in breast cancers must be addressed[J]. World Health Organization, 2013, 12.
2. Giordano SH, Kuo YK, Freeman JL, T. A. Buchholz, G. N. Hortobagyi, and J.S. Goodwin, “Risk of cardiac death after adjuvant radiotherapy for breast cancer,” J. Natl. Cancer Inst. 2005; 97, 419–424.
3. Harris EE, Correa C, Hwang WT, et al. Late cardiac mortality and morbidity in early-stage breast cancer patients after breast-conservation treatment. J Clin Oncol. 2006;24(25):4100-4106.
4. Hooning MJ, Botma A, Aleman BM, et al. Long-term risk of cardiovascular disease in 10-year survivors of breast cancer. J Natl Cancer Inst. 2007;99(5):365-375.
5. Marks LB, Yu X, Prosnitz RG, et al. The incidence and functional consequences of RT-associated cardiac perfusion defects. Int J Radiat Oncol Biol Phys. 2005;63(1):214-223.
6. Lind PA, Pagnanelli R, Marks LB, et al. Myocardial perfusion changes in patients irradiated for left-sided breast cancer and correlation with coronary artery distribution. Int J Radiat Oncol Biol Phys. 2003;55(4):914-920.
7. Huang JH, Wu XX, Lin X, Shi JT, Ma YJ, Duan S et al. Evaluation of fixed-jaw IMRT and tangential partial-VMAT radiotherapy plans for synchronous bilateral breast cancer irradiation based on a dosimetric study. J Appl Clin Med Phys. 2019; 20:9:31-41.
8. Tuomas V, Janne H, Kimmo M, Kristiina K, Topani L, Jan S. Tangential volumetric modulated arc therapy technique for left-sided breast cancer radiotherapy. Radiation Oncology (2015)10:79.
9. Yu PC, Wu CJ, Nien HH, Lui LT, Shaw S, Tsai YL. Tangent-based volumetric modulated arc therapy for advanced left breast cancer. Radiation Oncology. (2018)13:236.
10. Ares C, Khan S, MacArtain AM, Heuberger J, Goitein G, Gruber G, et al. Postoperative proton radiotherapy for localized and locoregional breast cancer: potential for clinically relevant improvements? Int J Radiat Oncol Biol Phys. (2010) 76:685–97.
11. Darby SC, McGale P, Taylor CW, Peto R. Long-term mortality from heart disease and lung cancer after radiotherapy for early breast cancer: prospective cohort study of about 300.000 women in US SEER cancer registries. Lancet Oncol. 2005; 6:557–565
12. Nilsson G, Holmberg L, Garmo H, Duvernoy O, Sjögren I, Lagerqvist B, et al. Distribution of coronary artery stenosis after radiation for breast cancer. J Clin Oncol. 2012;30:380–6.
13. Darby SC, Ewertz M, McGale P, Bennet AM, Blom-Goldman U, Brønnum D, et al. Risk of ischemic heart disease in women after radiotherapy for breast cancer. N Engl J Med. 2013;368:987–98.
14. Shah C, Badiyan S, Berry S, et al. Cardiac dose sparing and avoidance techniques in breast cancer radiotherapy. Radiother Oncol. 2014, 112:9–16.
15. Mast ME, Vredeveld EJ, Credoe HM, van Egmond J, Heijenbrok MW, Hug EB, et al. Whole breast proton irradiation for maximal reduction of heart dose in breast cancer patients. Br Cancer Res Treat. (2014) 148:33–9.
16. Tommasino F, Durante M, D’Avino V, Liuzzi R, Conson M, Farace P et al. Model-based approach for quantitative estimates of skin, heart, and lung toxicity risk for left-side photon and proton irradiation after breast-conserving surgery. Acta Oncologica, 2017, 56(5): 730-736.
17. Lomax AJ, et al. The clinical potential of intensity modulated proton therapy. Z Med Phys. 2004;14(3):147–52.
18. Lomax AJ. Intensity modulated proton therapy and its sensitivity to treatment uncertainties 1: the potential effects of calculational uncertainties. Phys Med Biol. 2008;53(4):1027–42.
19. Lomax AJ. Intensity modulated proton therapy and its sensitivity to treatment uncertainties 2: the potential effects of inter-fraction and interfiled motions. Phys Med Biol. 2008;53(4):1043–56.
20. Dowdell S, et al. Interplay effects in proton scanning for lung: a 4D Monte Carlo study assessing the impact of tumor and beam delivery parameters. Phys Med Biol. 2013;58(12):4137–56.
21. Knopf AC, Hong TS, Lomax A. Scanned proton radiotherapy for mobile targets-the effectiveness of re-scanning in the context of different treatment planning approaches and for different motion characteristics. Phys Med Biol. 2011;56(22):7257–71.
22. Unkelbach J, et al. Reducing the sensitivity of IMPT treatment plans to setup errors and range uncertainties via probabilistic treatment planning. Med Phys. 2009;36(1):149–63.
23. Liao L, Lim G J, Li Y, et al. Robust optimization for intensity modulated proton therapy plans with multi-isocenter large fields. International journal of particle therapy, 2016, 3(2): 305-311.
24. Ding X, et al. Spot-scanning proton arc (SPArc) therapy: the first robust and delivery-efficient spot-scanning proton arc therapy. Int J Radiat Oncol Biol Phys. 2016;96(5):1107–16.

25. Ding X, Li X, Qin A, Zhou J, Yan D, Stevens C, et al. Have we reached proton beam therapy dosimetric limitations? – a novel robust, delivery-efficient and continuous spot-scanning proton arc (SPArc) therapy is to improve the dosimetric outcome in treating prostate cancer. Acta Oncol. 2018;57(3):435–437.
26. Liu G, Li X, Qin A, Zheng W, Yan D, Zhang S, et al. Improve the dosimetric outcome in bilateral head and neck cancer (HNC) treatment using spot-scanning proton arc (SPArc) therapy: a feasibility study. Radiat Oncol. 2020 Jan 30;15(1):21.
27. Li X, Kabolizadeh P, Yan D, et al. Improve dosimetric outcome in stage III non-small-cell lung cancer treatment using spot-scanning proton arc (SPArc) therapy. Radiat Oncol. 2018;13:35.
28. Ding X, Zhou J, Li X, et al. Improving dosimetric outcome for hippocampus and cochlea sparing whole brain radiotherapy using spot-scanning proton arc therapy. Acta Oncol. 2019;58:483–490.
29. Breast Cancer Atlas for Radiation Therapy Planning: Consensus Definitions (2017).
30. Shaitelman SF, et al. Acute and short-term toxic effects of conventionally fractionated vs Hypofractionated whole-breast irradiation: A Randomized Clinical Trial. JAMA Oncol. 2015;1(7):931-941.
31. Whelan TJ et al. Long-term results of hypofractionated radiation therapy for breast cancer. N Engl J Med 2010;362:513-520.
32. Quan EM, Li X, Li Y, Wang X, Kudchadker RJ, Johnson JL, et al. A comprehensive comparison of IMRT and VMAT plan quality for prostate Cancer treatment. Int J Radiat Oncol. 2012;83:1169–
33. Liu W, et al. Effectiveness of robust optimization in intensity-modulated proton therapy planning for head and neck cancers. Med 2013; 40(5):051711.
34. Kardar L, et al. Evaluation and mitigation of the interplay effects of intensity modulated proton therapy for lung cancer in a clinical setting. Pract Radiat Oncol. 2014;4(6):e259–68.
35. Kallman P, Agren A, Brahme A: Tumour and normal tissue responses to fractionated non-uniform dose delivery. Int J Radiat Biol 1992, 62:249–262.
36. Pastore F, Conson M, D'avino V, et al. Dose-surface analysis for prediction of severe acute radio-induced skin toxicity in breast cancer patients. Acta Oncol. 2016;55:466–473.
37. Seppenwoolde Y, Lebesque JV, de Jaeger K, Belderbos JS, Boersma LJ, Schilstra C, Henning GT, Hayman JA, Martel MK, Ten Haken RK: Comparing different NTCP models that predict the incidence of radiation pneumonitis. Int J Radiat Oncol Biol Phys. 2003, 55: 724-735.
38. Lyman JT: Complication probability as assessed from dose-volume histograms. Radiat Res Suppl 1985, 8:S13–S19.
39. Gagliardi G, Lax I, Ottolenghi A, Rutqvist LE. Long-term cardiac mortality after radiotherapy of breast cancerdapplication of the relative seriality model. Br J Radiol. 1996;69:839-846.
40. Koschik A, Bula C, Duppich J, et al. Gantry 3: further development of the psi proscan proton therapy facility; Proceedings of IPAC 2015, Richmond, VA, USA TUPWI016.
41. Michalski A, Atyeo J, Cox J, Rinks M. Inter- and intra-fraction motion during radiation therapy to the whole breast in the supine position: a systematic review. J Med Imaging Radiat Oncol. 2012;56(5):499–509.
42. Miller D, Klein E, Zoberi I, Taylor M, Powell S. Inter-fraction and intra-fraction breast motion localized using AlignRT for early breast cancer. Int J Radiat Oncol Biol Phys 2008; 72: S189–90.
43. Lee J, Liu SH, Lin JB, et al. Image-guided study of inter-fraction and intra-fraction set-up variability and margins in reverse semi-decubitus breast radiotherapy. Radiat Oncol. 2018;13(1):254.
44. Taylor AM, Wang Z, Macaulay E, Jagsi R, Duane F, Darby SC. Exposure of the heart in breast cancer radiotherapy: a systematic review of heart doses published during 2003–2013. Int J Radiat Oncol Biol Phys. (2015) 93:845–53.
45. Rehammar JC, Jensen MB, McGale P, et al. Risk of heart disease in relation to radiotherapy and chemotherapy with anthracyclines among 19,464 breast cancer patients in Denmark, 1977–2005. Radiother Oncol. 2017;123:299–305.
46. Henson K E, McGale P, Parkin D M, et al. Cardiac mortality after radiotherapy, chemotherapy and endocrine therapy for breast cancer: Cohort study of 2 million women from 57 cancer registries in 22 countries. Int J Cancer. 2020;10.1002/ijc.32908.
47. Jacob, S., Camilleri, J., Derreumaux, S. et al. Is mean heart dose a relevant surrogate parameter of left ventricle and coronary arteries exposure during breast cancer radiotherapy: a dosimetric evaluation based on individually-determined radiation dose (BACCARAT study). Radiat Oncol 14, 29 (2019).

48. Becker-Schiebe, M., Stockhammer, M., Hoffmann, W. et al. Does mean heart dose sufficiently reflect coronary artery exposure in left-sided breast cancer radiotherapy?. Strahlenther Onkol 192, 624–631 (2016).
49. Bekelman JE, Lu H, Pugh S, et al. Pragmatic randomised clinical trial of proton versus photon therapy for patients with non-metastatic breast cancer: the Radiotherapy Comparative Effectiveness (RadComp) Consortium trial protocol. BMJ Open. 2019;9(10):e025556.
50. van den Bogaard VA, Ta BD, van der Schaaf A, Bouma AB, Middag AM, Bantema-Joppe EJ, et al. Validation and modification of a prediction model for acute cardiac events in patients with breast Cancer treated with radiotherapy based on three-dimensional dose distributions to cardiac substructures. J Clin Oncol. (2017) 35:1171–8.
51. Jimenez RB, Goma C, Nyamwanda J, Kooy HM, Halabi T, Napolitano BN, et al. Intensity modulated proton therapy for postmastectomy radiation of bilateral implant reconstructed breasts: a treatment planning study. Radiother Oncol. (2013) 107:213–7.
52. Xu N, Ho MW, Li Z, Morris CG, Mendenhall NP. Can proton therapy improve the therapeutic ratio in breast cancer patients at risk for nodal disease? Am J Clin Oncol. (2014) 37:568–74.
53. MacDonald SM, Patel SA, Hickey S, Specht M, Isakoff SJ, Gadd M, et al. Proton therapy for breast cancer after mastectomy: early outcomes of a prospective clinical trial. Int J Radiat Oncol Biol Phys. (2013) 86:484–90.

Figures

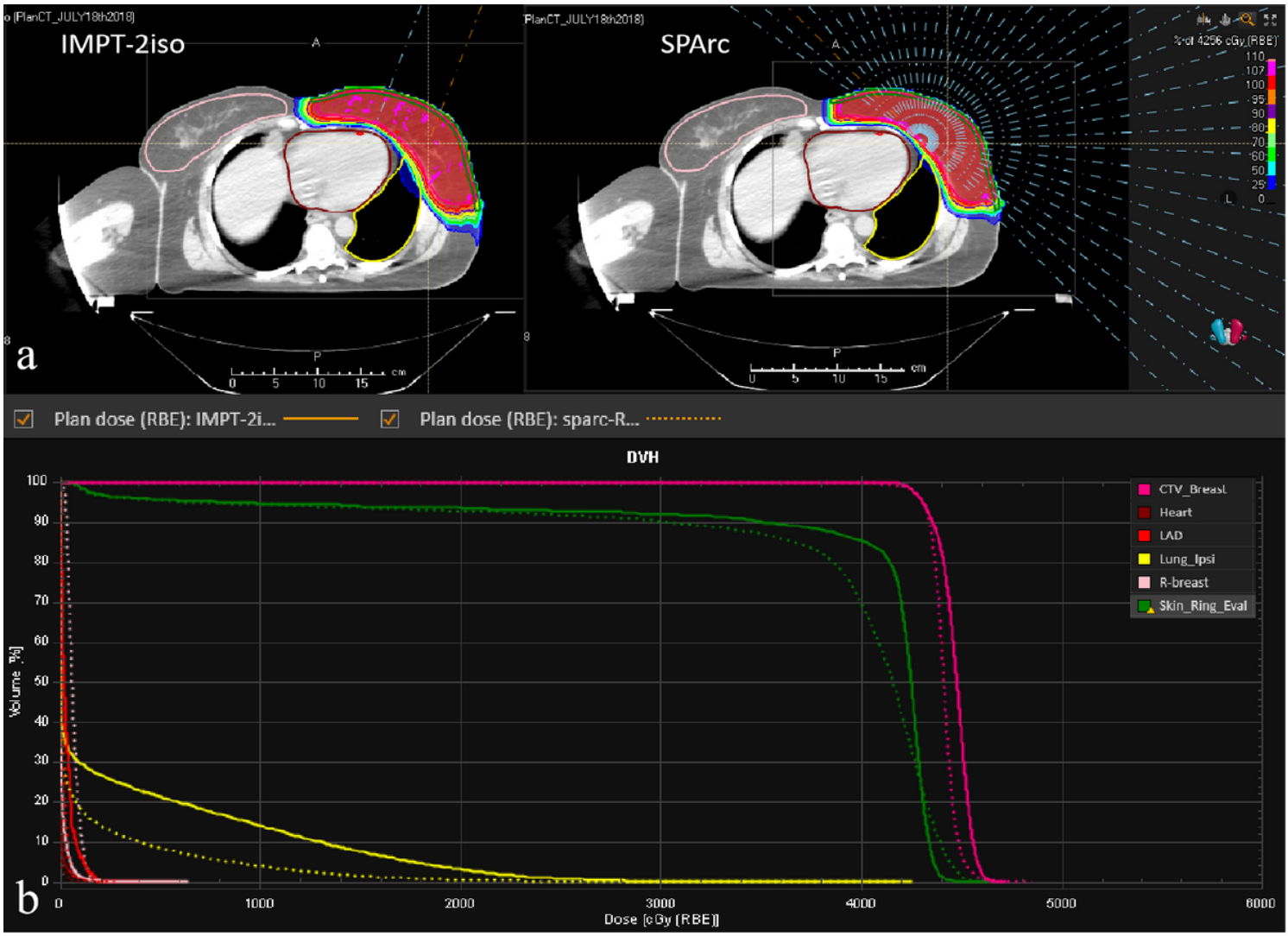

Figure 1

A representative of the radiation treatment plan from case #5. The comparison of (a) patient dose distribution, beam angle and (b) dose volume histograms (DVHs) (solid and dash lines for vIMPT and SPArc).

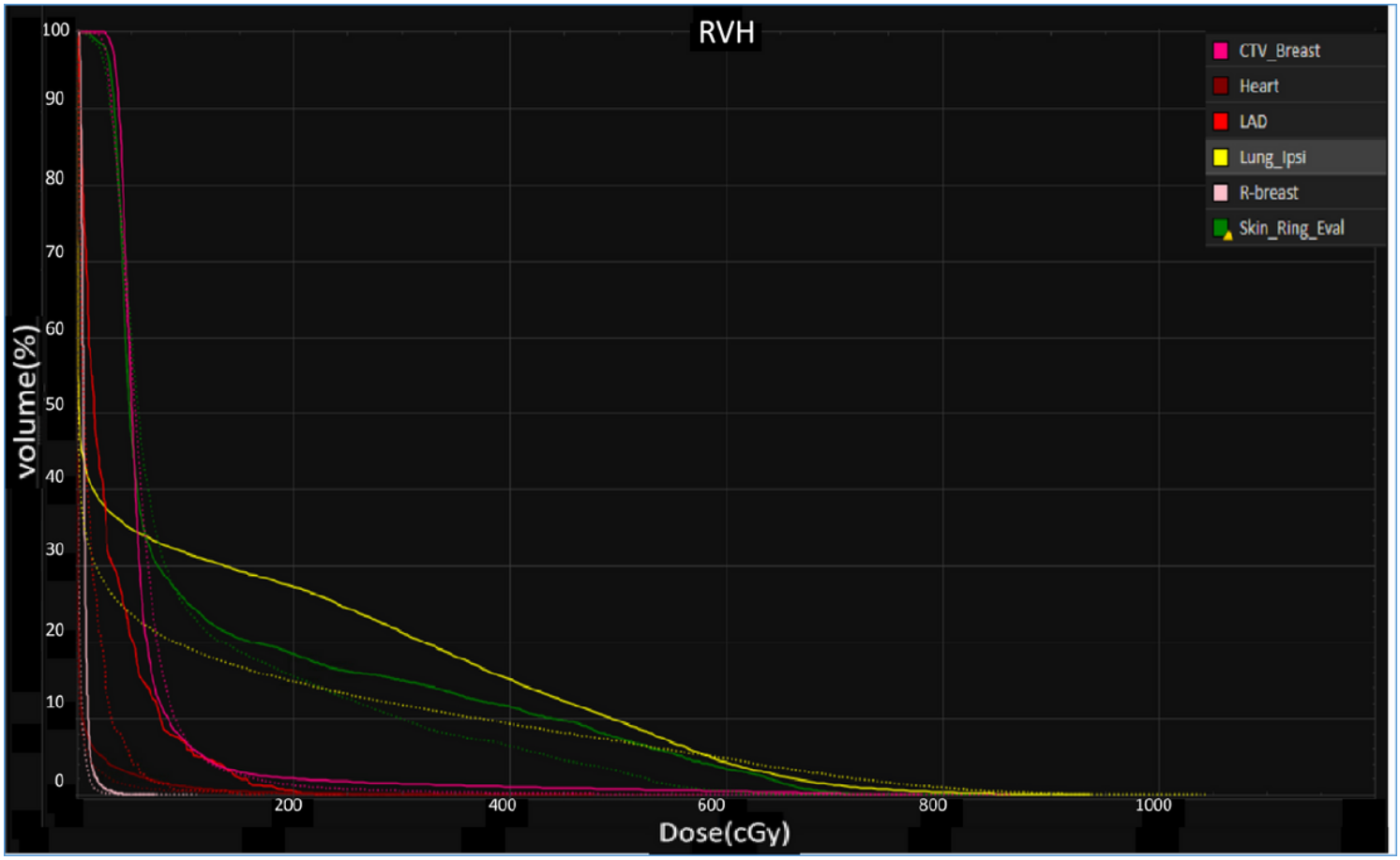

Figure 2

Root-mean Square Dose volume Histogram (RVH) of different OARs. The solid line is vIMPT and the dashed line is SPArc (case #5).

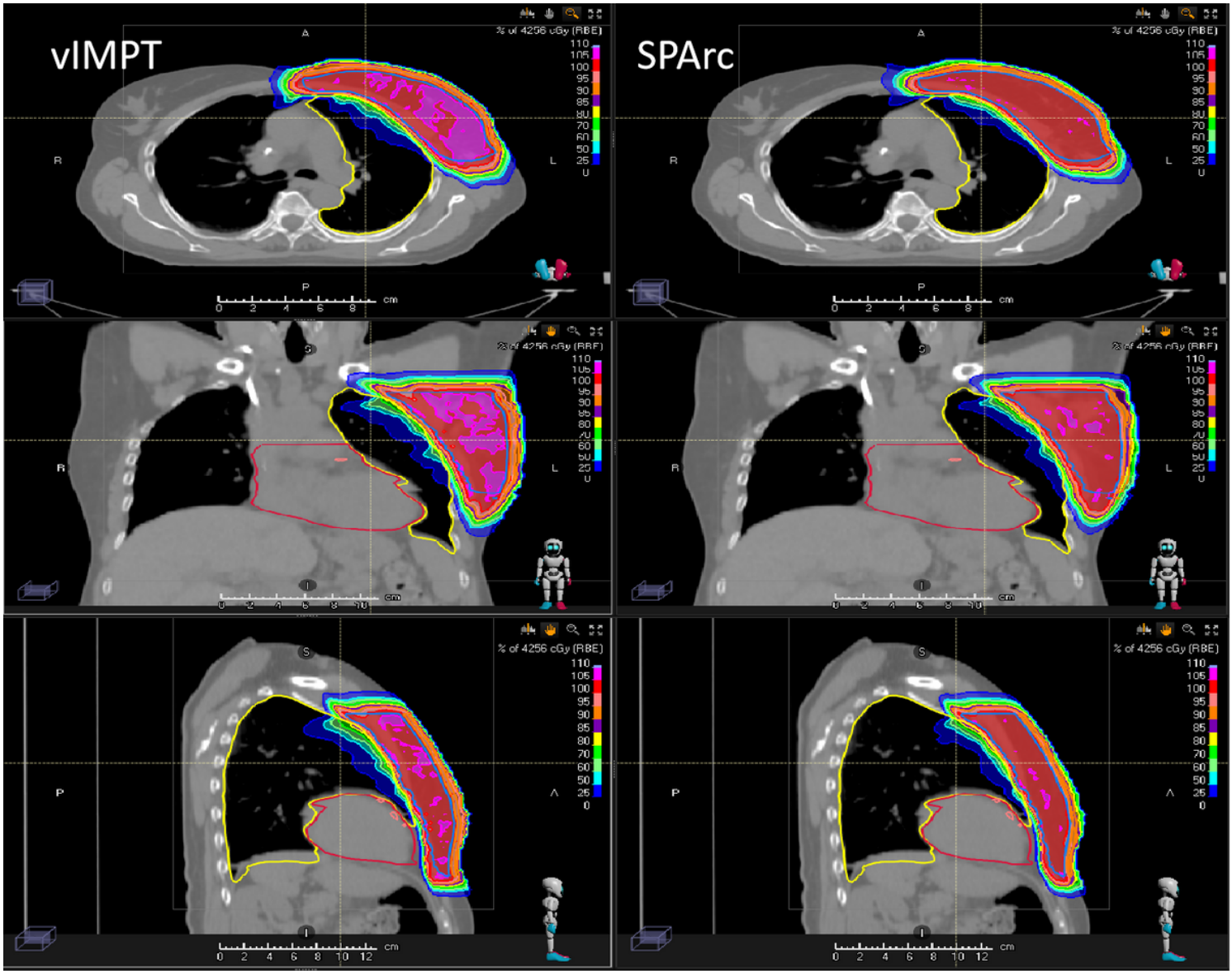

Figure 3

The single-fraction 4D dynamic dose distributions on phase (CT50) for vIMPT and SPArc.

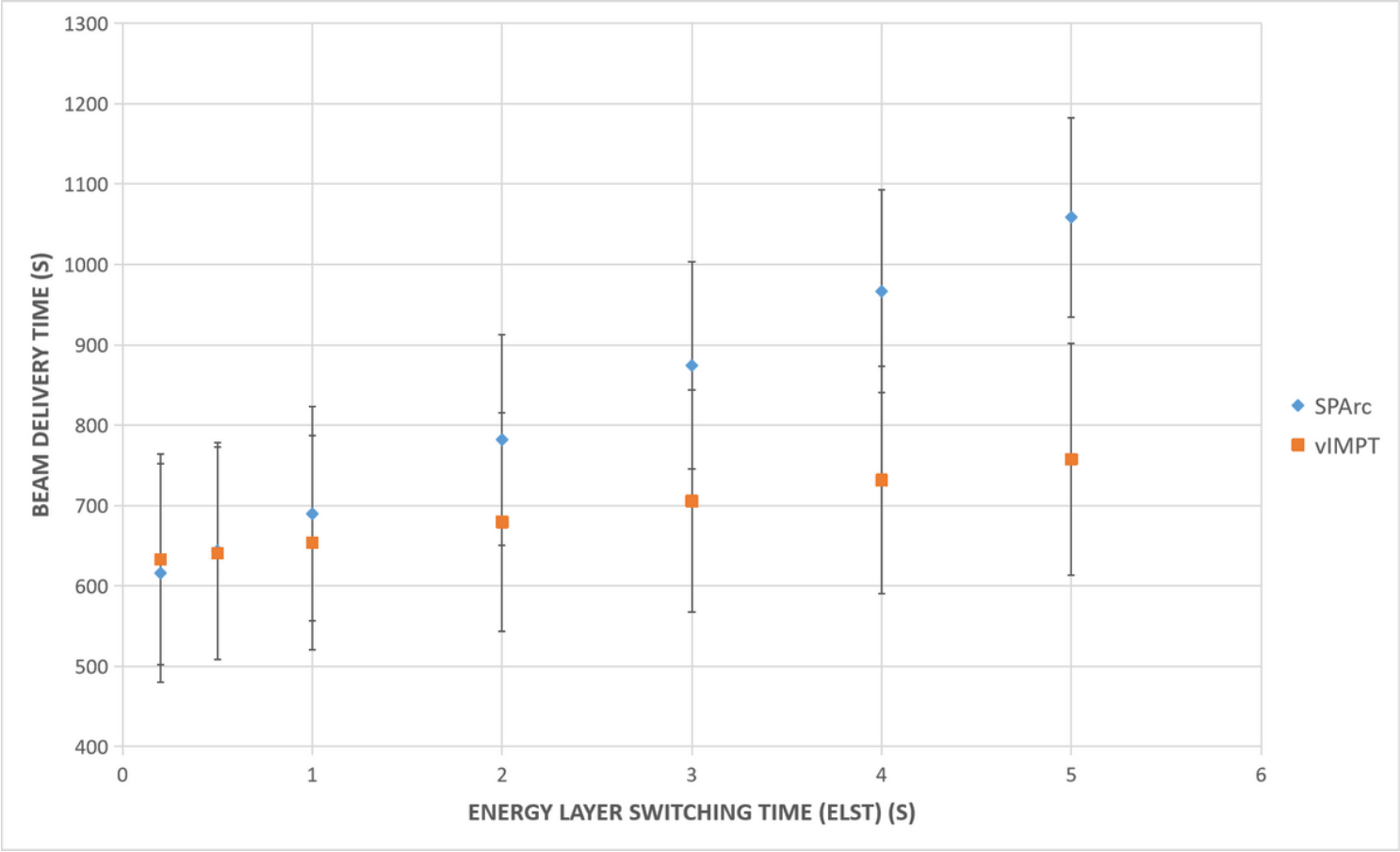

Figure 4

Total average treatment beam delivery time.

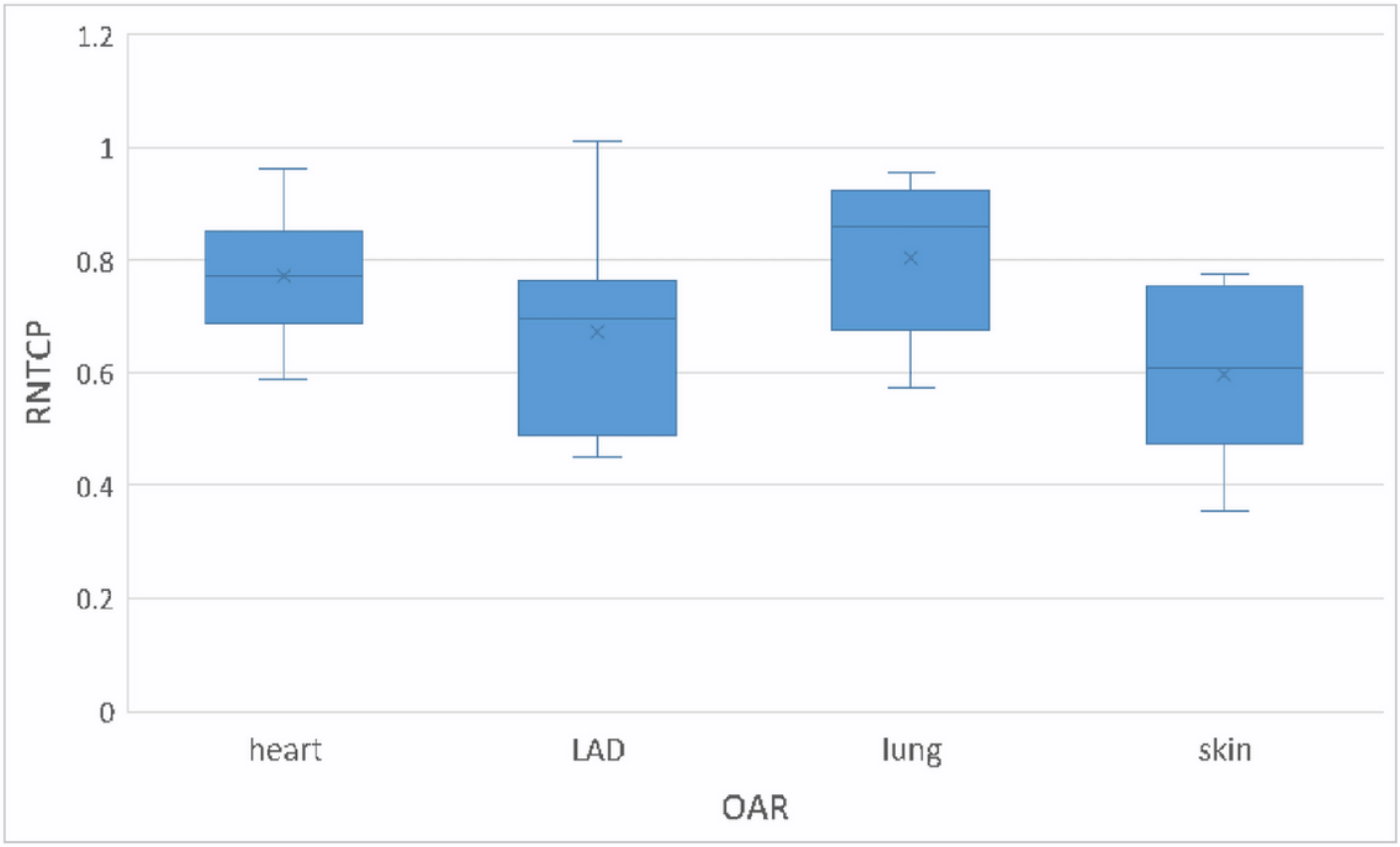

Figure 5

Box-whisker plot of RNTCP comparison according to NTCP analysis for heart, LAD, skin and lung.